Pergamon

Tetrahedron 56 (2000) 9409–9419

TETRAHEDRON

High Level Production, Characterization and Construct Optimization of the Ionotropic Glutamate Receptor Ligand Binding Core

Guo Qiang Chen* and Eric Gouaux*

Department of Biochemistry and Molecular Biophysics, Columbia University, 650 West 168th Street, New York, NY 10032, USA

Received 17 February 2000; accepted 28 July 2000

Abstract—Multimilligram quantities of active and pure GluR2-S1S2, the recombinant ligand binding core of the AMPA-sensitive GluR2 receptor, were produced by preparative folding of the solubilized inclusion bodies expressed in 1 l of *Escherichia coli* cell culture. The biochemical properties and biological activities of folded protein were characterized and the protein construct was optimized for three-dimensional structural studies.

Introduction

Multimilligram quantities of active, stable and pure protein are prerequisites for many detailed biochemical, pharmaceutical and structural studies. Unfortunately, high level production of eukaryotic proteins from either natural or recombinant sources is often difficult. This paper describes how protein engineering and biochemical approaches were employed to produce large quantities of the glutamate receptor ligand binding core GluR2-S1S2, to characterize the protein folding products, and to optimize the protein construct for structural and functional studies.

The ionotropic glutamate receptors (iGluRs), found mainly in the central nervous system, are ligand-gated ion channels that mediate neurotransmission in vertebrates and invertebrates.[1] iGluRs are found throughout the nervous system and they mediate higher brain functions such as learning and memory. In addition to the essential roles of iGluRs in normal neurophysiology, dysfunctional receptors are implicated in brain diseases and neurologic disorders such as epilepsy, and in Parkinson's and Alzheimer's diseases.[2,3]

Binding of an agonist to an iGluR opens the cation permeable ion channel and the resulting ion flux depolarizes the cell and initiates a synaptic potential.[1] Based on their affinities and functional responses to agonists, iGluRs have been classified into three groups: GluR1-4 are the AMPA (α-amino-3-hydroxy-5-methylisoxazole-4-propionic acid) receptors; NMDAR1, NMDAR2a-d and NMDAR3a belong to the *N*-methyl-D-aspartate (NMDA) class; and GluR5-7 and KA1-2 comprise the kainate receptors.[4–7]

iGluRs have a so-called S1S2 extracellular region which functions in ligand binding and a membrane-embedded domain which comprises the ion channel.[8–11] In addition to the S1S2 ligand binding region, there is a glycosylated N-terminal domain (ATD) of approximately 400 residues. Although the biological function of the ATD is not well understood, it appears to modulate the properties of the ion channel and participate in subunit assembly.[1,12,13] As shown in Fig. 1, the ligand binding domain of GluR2 is composed of two extracellular segments S1 and S2 which are separated by transmembrane regions M1 and M2 and the reentrant loop P.

The first functional recombinant ligand binding core of GluR2 was designed by Kuusinen et al. using a 13-residue linker to connect the S1 and S2 regions.[14] Low level expression of this construct was achieved in insect cells and subsequently in the periplasm of *Escherichia coli* cells.[15] Based on this GluR2-S1S2 construct, we designed a similar construct specifically for expression of GluR2-S1S2 as inclusion bodies in *E. coli* cells.[16] Our GluR2-S1S2 gene was cloned into pETGQ, a modified pET30b expression vector, and was over-expressed as a His-tagged protein (HS1S2) in the form of inclusion bodies. HS1S2 was solubilized, purified and folded using a fractional factorial folding screen. The folded HS1S2 was further purified to homogeneity and its biochemical, biophysical and ligand binding properties were analyzed.[16] Limited proteolysis of the folded HS1S2 suggested that sequences in the terminal regions of S1 and S2 and in the linker region were not only

Keywords: glutamate receptor; ligand binding; *Escherichia coli*; protein production; protein engineering; preparative folding; X-ray crystallography.
* Corresponding authors. Tel.: +212-305-4062;
e-mail: gc167@columbia.edu;
Tel.: +212-305-4475; fax: +212-305-8174; e-mail: jeg52@columbia.edu

0040–4020/00/$ - see front matter
PII: S0040-4020(00)00825-5

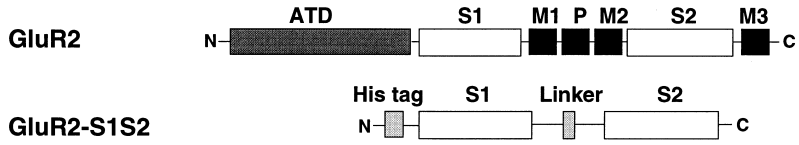

Figure 1. Schematic representation of the full-length GluR2 and the recombinant ligand binding domain GluR2-S1S2. N and C represent the amino and carboxyl termini of the protein construct, respectively. ATD is the amino terminal domain of the full length GluR2. S1 and S2 comprise the ligand binding domain. The transmembrane regions include M1, M2 and M3. P represents the reentrant loop of the ion channel. The His tag sequence was MHHHHHHHHSSGLVPRGSAMG. The linker sequences are described in the text.

flexible but were also not essential for ligand binding. On the basis of limited proteolysis data and sequence alignment analysis, a series of ligand binding core constructs was designed.[17] Over expression, in vitro folding and purification of the shortest construct that was active in ligand binding (HS1S2I) yielded 45 mg of purified monomeric protein from 1 l of *E. coli* culture. The folded HS1S2I construct retained ligand binding activity, possessed good biochemical behavior and produced crystals that diffracted to 1.6 Å resolution.[18] We hope that the strategies used for the high level production, characterization and construct optimization of GluR2-S1S2 presented here may be applied to other glutamate receptors or receptor domains.

Results

Over-expression and purification of HS1S2

HS1S2 was over-expressed from the pHS1S2 plasmid in BL21(DE3) cells after induction of the host cells with 1 mM IPTG at 37°C for 2 h. The insoluble inclusion bodies were isolated from the cell lysate by a low speed centrifugation step. Soluble impurities and some cell membrane-associated materials were removed from the inclusion bodies during the 2 cycles of resuspension and centrifugation. At this stage, HS1S2 comprised approximately 80% of the inclusion body protein, as judged by sodium dodecyl sulfate-polyacrylamide gel electrophoresis (SDS-PAGE). An additional level of purification was achieved by dialysis of the solubilized inclusion bodies against Buffer A (20 mM NaOAc, 4 M GuHCl, 1 mM EDTA, 1 mM DTT, pH 4.5) which resulted in the precipitation of some of the contaminating proteins. After the dialysis step, about 90% of the solubilized protein was monomer, according to analytical size exclusion chromatography (SEC). Preparative SEC in Buffer A yielded about 100 mg of ca. 90% pure HS1S2 per liter of culture.

Protein solubility

The following three methods were applied to analyze the folding reactions: SDS-PAGE for protein solubility, SEC for protein aggregation state, and ligand binding experiments for protein activity. After dialysis of the unfolded monomeric HS1S2 against the folding buffers (Table 1), misfolded and aggregated protein precipitated from solution and the precipitate was removed by centrifugation. On the basis of SDS-PAGE results, the yields of soluble HS1S2 were ~20% for conditions 2, 3, 13, 15, ~10% for conditions 4, 8, 10, and ≤3% for the remaining conditions.

Protein aggregation state

Among the 4 folding conditions (2, 3, 13 and 15) that gave the most soluble HS1S2, 3 conditions (2, 13 and 15) yielded 5–10% monomer, as estimated by SEC. Fig. 2 illustrates the FPLC and HPLC traces for the folding mixture under condition 2. Analysis of the folding reaction mixture on a Superose 12 column in Buffer B (20 mM Tris-HCl, pH 7.4, 1 mM EDTA, 200 mM NaCl) showed both monomeric and highly aggregated forms (>1000 kDa). About one third of the soluble protein was folded monomer according to the FPLC result. Analysis of the reaction mixture by HPLC using a TSK-GEL G3000SW column in buffer F (0.1 M sodium phosphate, pH 6.8, 200 mM Na_2SO_4, 1 mM DTT, 10 mM glutamate, 2 mM EDTA) showed the monomer fraction while the aggregated material adhered to the resin. In contrast to the behavior of HS1S2 under folding condition 2, the majority of the protein folded under condition 3 was aggregated and the monomer yield was <0.1%.

Receptor ligand binding activity

The ligand binding activity of the folded HS1S2 was demonstrated by specific binding of ^{3}H AMPA and by competitive inhibition of ^{3}H AMPA binding by cold glutamate and kainate. The ligand binding experiments showed that the folding conditions that gave the highest yield of monomer (2, 13, 15) also produced the highest ligand binding activity. Using the folded and purified protein, the ^{3}H AMPA K_d and the glutamate and kainate IC_{50} values were measured (Fig. 3). The K_d of AMPA binding was 23±5.3 nM while the IC_{50} values for glutamate and kainate were 116±56 nM and 1.9±1.2 μM, respectively. The ligand binding properties of HS1S2 were roughly comparable to those obtained from GluR2-S1S2 expressed in the periplasm of *E. coli* (AMPA K_d=11 nM, glutamate IC_{50}=370 nM, kainate IC_{50}=3.3 μM).[15]

Spectroscopic properties

Folded HS1S2 possessed α and β secondary structure as judged by its circular dichroism (CD) spectrum (Fig. 4A). By contrast, HS1S2 in 4 M GuHCl had a CD spectrum corresponding to random coil. Estimation of the secondary structure content from the CD data using the k2d software[19,20] resulted in a prediction of 35% α-helix for HS1S2. Changes in tryptophan and tyrosine fluorescence of HS1S2I upon ligand binding suggested that a conformational change occurs upon complex formation. For example, binding of glutamate or kainate resulted in a red shift of the maximum emission wavelength from 331 to 332 nm. The fluorescence emission intensity at 331 nm increased 3.8%

Table 1. Fractional factorial folding screen for the folding of HS1S2

#[a]	Pattern[b]	Conditions												Analysis		
		Protein (mg/ml)	pH	IS[c] (mM)	T[d]	Divalents[e]	Polar additive	Nonpolar additive[f]	Chaotrope	Red./Ox.[g]	Detergent[h]	Ligand[i]	PEG[j]	SDS-PAGE[k]	SEC[l] (%)	Ligand Binding[m]
1	−+−++−+−−+−+	0.1	8.5	10	20	Mg,Ca	None	21%	None	DTT	5.0 mM	None	0.05%	−	1.0	782
2	++++−−−−−−−+	1.0	8.5	250	4	EDTA	None	None	None	DTT	None	None	0.05%	++	6.0	8318
3	−+++−+−+−+−−	0.1	8.5	250	20	EDTA	0.5 M Arg	None	0.75 M GuHCl	DTT	5.0 mM	None	None	++	<0.1	< 200
4	−+−−−+−++−++	0.1	8.5	10	4	EDTA	0.5 M Arg	None	0.75 M GuHCl	GSH:GSSG	None	10.0 mM	0.05%	+	<0.1	< 200
5	+−+−++−−+−+−	1.0	6.0	250	4	Mg,Ca	0.5 M Arg	None	None	GSH:GSSG	5.0 mM	None	None	−	1.0	< 200
6	+−++−−++−−+−	1.0	6.0	250	20	EDTA	None	21%	0.75 M GuHCl	DTT	None	10.0 mM	None	−	0.4	< 200
7	++++++++++++	1.0	8.5	250	20	Mg,Ca	0.5 M Arg	21%	0.75 M GuHCl	GSH:GSSG	5.0 mM	10.0 mM	0.05%	−	0.8	< 200
8	−−−−+−−+−++−	0.1	6.0	10	4	Mg,Ca	None	None	0.75 M GuHCl	DTT	5.0 mM	10.0 mM	None	+	4.0	2891
9	+−−++−−−−++	1.0	6.0	10	20	Mg,Ca	0.5 M Arg	None	None	DTT	None	10.0 mM	0.05%	−	0.6	< 200
10	−−+−−++−−+++	0.1	6.0	250	4	EDTA	0.5 M Arg	21%	None	DTT	5.0 mM	10.0 mM	0.05%	+	3.0	< 200
11	−−+++−−+−−+	0.1	6.0	250	20	Mg,Ca	None	None	0.75 M GuHCl	GSH:GSSG	None	None	0.05%	−	<0.1	< 200
12	+−−−−−+++−+	1.0	6.0	10	4	EDTA	None	21%	0.75 M GuHCl	GSH:GSSG	5.0 mM	None	0.05%	−	1.0	< 200
13	++−−+++−−−−	1.0	8.5	10	4	Mg,Ca	0.5 M Arg	21%	0.75 M GuHCl	DTT	None	None	None	++	5.0	5490
14	++−+−−−−+++−	1.0	8.5	10	20	EDTA	None	None	None	GSH:GSSG	5.0 mM	10.0 mM	None	−	0.3	< 200
15	−++−+−+−+−+−	0.1	8.5	250	4	Mg,Ca	None	21%	None	GSH:GSSG	None	10.0 mM	None	++	8.0	6183
16	−−−+−++−+−−−	0.1	6.0	10	20	EDTA	0.5 M Arg	21%	None	GSH:GSSG	None	None	None	−	<0.1	<200

[a] Solution number.
[b] Pattern of factor levels.
[c] Ionic strength, molar ratio of NaCl to KCl was 25:1.
[d] T was temperature in °C.
[e] $MgCl_2$, $CaCl_2$ concentrations were 2 mM, EDTA concentration was 1.0 mM.
[f] The nonpolar additive was composed of 20% glycerol (v/v) and 1% sucrose (w/v).
[g] Concentration of DTT was 1.0 mM and the concentrations of reduced (GSH) and oxidized (GSSG) glutathione were 1.0 mM and 0.1 mM, respectively.
[h] DiC_7PC.
[i] L-Glutamate.
[j] PEG MWave=3350 Da and the concentration was w/v.
[k] Protein concentration in the supernatant following dialysis against refolding buffers and centrifugation at 128000×g for 30 min (4°C) was estimated by SDS PAGE. The '−' corresponds to <0.1 μg or to <3% yield of water-soluble HS1S2 while '+' and '++' correspond to ~10% and ~20% yields of water-soluble HS1S2, respectively.
[l] Folding yield estimated by integration of monomer peak from SEC chromatogram.
[m] The units are cpm. ^{3}H-AMPA (20 nM, 10.6 Ci/mmole) and 2 μl or 20 μl of each refolding mixture with an initial protein concentration of 1.0 mg/ml or 0.1 mg/ml, respectively, were used to measure specific ligand binding as described in the Experimental section.

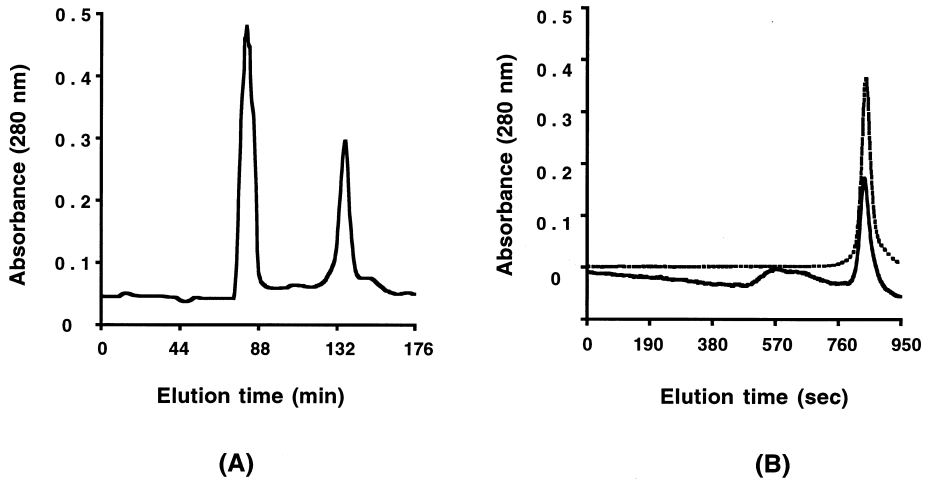

Figure 2. Size exclusion chromatography (SEC) of HS1S2 following folding using condition #2 from the 16 condition screen (Table 1). (A) FPLC SEC of the folding reaction mixture on a Superose 12 column in Buffer B. (B) HPLC SEC of the folding mixture on a TSK-GEL G3000SW column in buffer F. The dashed line is a SEC trace of purified folded HS1S2 under the same chromatographic conditions. The absorbance units are arbitrary.

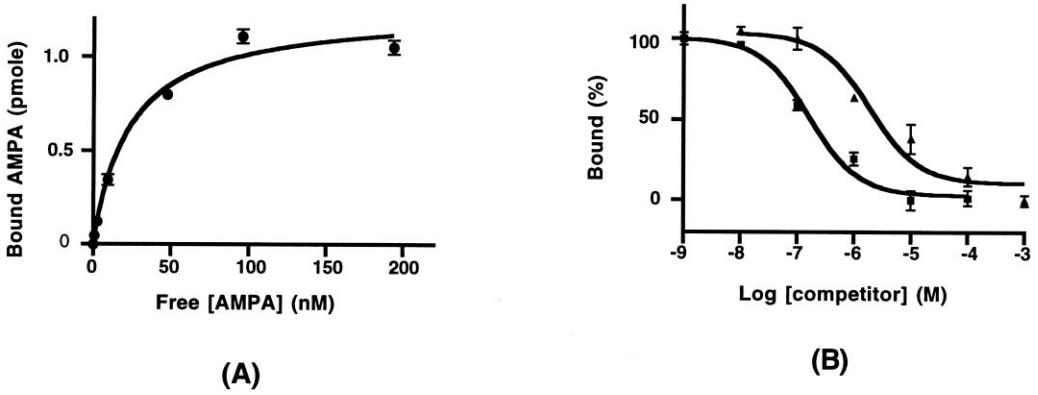

Figure 3. The ligand binding activity of folded HS1S2. (A) K_d measurement by saturation binding of AMPA. The K_d value was 23±5.3 nM. (B) Competition binding of glutamate (■) and kainate (▲). The IC_{50} values for glutamate and kainate were 116±56 nM and 1.9±1.2 μM, respectively.

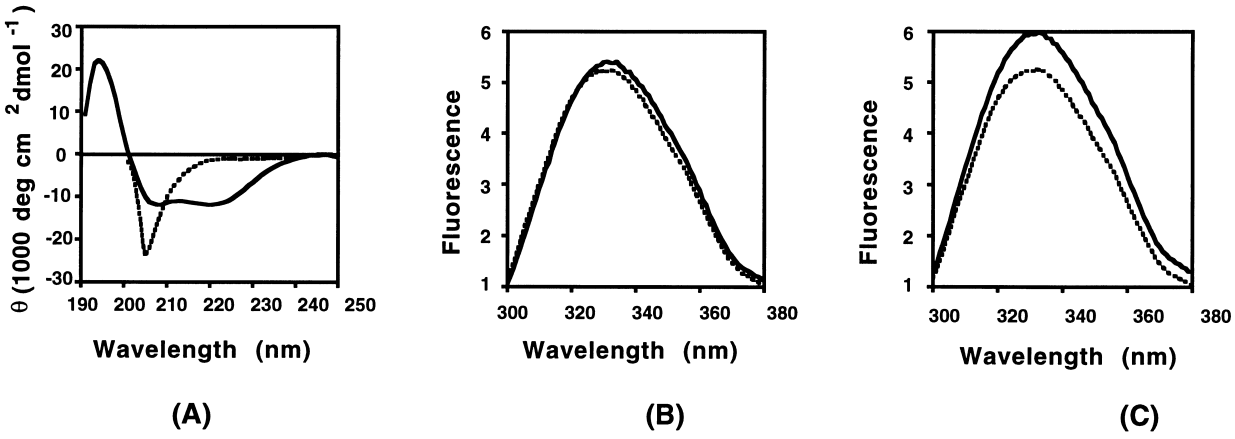

Figure 4. Spectral analysis of the folded GluR2-S1S2. (A) Circular dichroism (CD) spectra of the folded HS1S2 in Buffer B (solid line) and the unfolded protein in Buffer A (dashed line). Fluorescence emission spectra of folded HS1S2I in the presence of glutamate (B, solid line) and kainate (C, solid line). The dashed line is the spectrum the apo protein. The fluorescence units are arbitrary. The λ_{max} for the apo protein was 331 nm. The λ_{max} for the glutamate or kainate-bound protein was 332 nm.

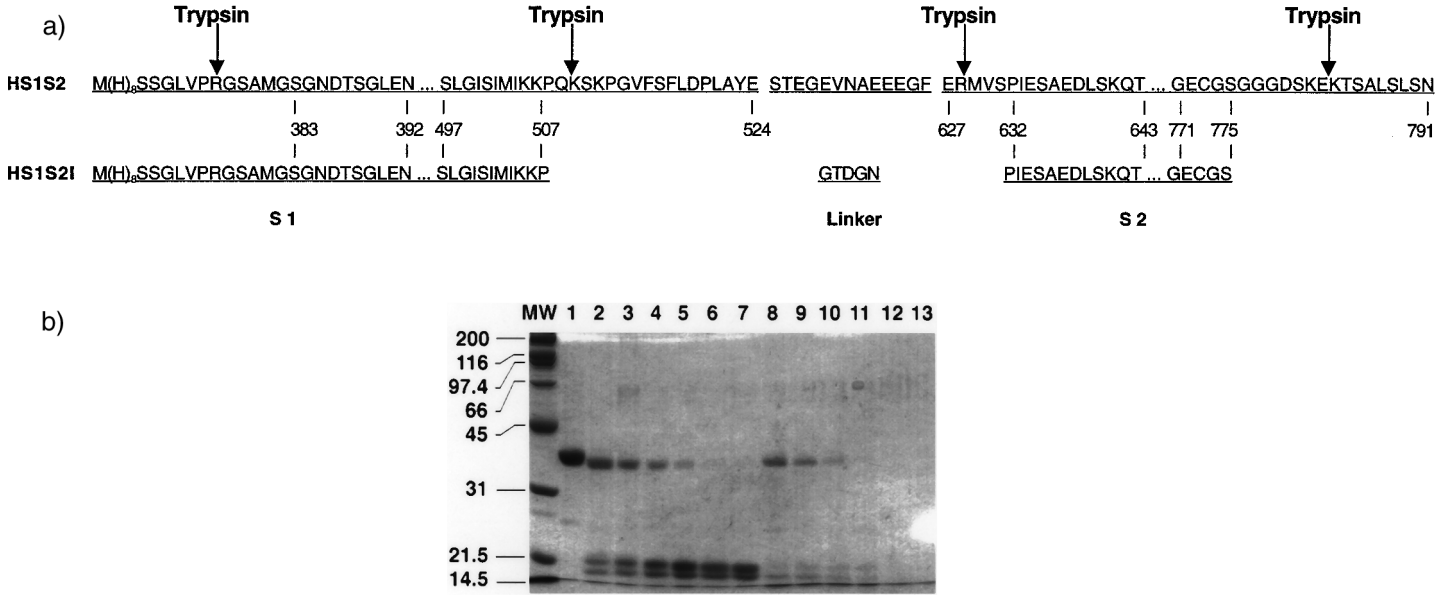

Figure 5. (A) Regions of the amino acid sequences of HS1S2 (upper) and HS1S2I (lower) which contain sites of trypsin cleavage. In HS1S2I, the only site that is cleaved by trypsin is the first site, seven residues downstream of the histidine tag. (B) SDS-PAGE of trypsinolysis of HS1S2 in the presence or absence of glutamate. Lane 1, HS1S2 without trypsin digestion; lanes 2–7, reactions in the presence of 2 mM glutamate with digestion times 5, 10, 20, 30, 45, and 60 min, respectively; lanes 8–13, the same reaction conditions as lanes 2–7 but without glutamate in the reaction mixture.

Table 2. Fractional factorial folding screen for the folding of HS1S2I

#[b]	Pattern[c]	Conditions[a]					Analysis
		pH	[NaCl] (mM)	[KCl] (mM)	Arg (M)	GuHCl (M)	AMPA binding[d] (1000 cpm)
1A	−−−−	7	10	0.4	0.0	0.0	2.2
2A	−−++	7	10	0.4	0.65	0.5	55.9
3A	−+−+	7	250	10	0.0	0.5	12.0
4A	−++−	7	250	10	0.65	0.0	3.3
5A	+−−+	8.5	10	0.4	0.0	0.5	7.3
6A	+−+−	8.5	10	0.4	0.65	0.0	65.1
7A	++−−	8.5	250	10	0.0	0.0	61.0
8A	++++	8.5	250	10	0.65	0.5	52.2

[a] The common solution condition was 20 mM Tris–HCl, 1 mM EDTA, 1.0 mg/ml HS1S2I, 4°C.
[b] Solution number.
[c] Pattern of factor levels.
[d] The ligand binding reactions were composed of 4 μl of the dialyzed reaction mixture, 470 μl of Buffer G and 25 μl of 1: 4 ^{3}H:^{1}H AMPA. The nonspecific binding control reactions contained 1 mM glutamate. Typically, the nonspecific binding controls gave about 300 cpm.

for glutamate binding and 13.9% for kainate binding (Fig. 4B and 4C).

Limited proteolysis

There are over 30 potential trypsin sites within the HS1S2 construct. Limited trypsin digestion of HS1S2 combined with SDS-PAGE and N-terminal sequencing revealed the four most accessible sites: the thrombin/trypsin site after the His tag, K_{509} in the C-terminal region of S1, R_{628} at the N-terminus of S2, and K_{783} in the C-terminal area of S2 (Fig. 5A). MALDI-MS analysis was used to define the C-termini of the trypsin fragments, showing that the major digestion products $GSAMGS_{383}$–R_{628} (17.8 kDa), M_{629}–K_{783} (17.1 kDa) and $GSAMGS_{383}$–K_{509} (14.5 kDa). The extra amino acid sequence GSAMG before S_{383} was due to the DNA sequences for the thrombin and NcoI sites. Inclusion of 2 mM glutamate in the reaction mixtures inhibited the digestion reactions (Lane 2–7, Fig. 5B) compared to the reactions without glutamate (Lane 8–13, Fig. 5B).

Protein construct optimization

A construct of GluR2-S1S2, named HS1S2I, was designed on the basis of multiple sequence alignments of eukaryotic iGluRs and bacterial periplasmic ligand binding proteins, and on the basis of limited proteolysis data. Multiple sequence alignment of GluR1-7 revealed that N_{392}, P_{507}, P_{632}, and W_{767} of GluR2 are conserved residues in the iGluR family. Sequence alignment with bacterial periplasmic ligand binding proteins such as glutamine binding protein (QBP) showed that the prokaryotic proteins do not have the sequences corresponding to Q_{508}–E_{524} and W_{766}–N_{791} of GluR2.[21] The similarity between GluR2-S1S2 and QBP on the three-dimensional structure level was shown by their crystal structures.[18] In addition, the proteolysis results suggested that K_{509}, the linker region, and R_{628} and K_{783} were the most protease-accessible sites. Therefore, in the new HS1S2I construct, sequences between Q_{508}–E_{524}, E_{627}–S_{631} and G_{776}–N_{791} were deleted (Fig. 5A). Finally, the 13 residue linker was shortened to a 5 residue linker (GTDGN) derived from a 3:5 β-turn in concanavalin A.[22]

The expression level of HS1S2I in BL21(DE3) cells was similar to that of HS1S2. On the basis of the folding screen results for the HS1S2 construct, a new folding screen was applied to the folding of HS1S2I. This higher resolution screen focused on pH and the concentrations of glycerol, arginine and salt (Table 2). In this 8 experiment screen, condition 6A gave the highest yield (15–20%) of active, monomeric protein. Protein that precipitated during the folding was collected by centrifugation and recycled, thus raising the total yield of monomeric HS1S2I to ~45% after three folding reactions. The portion of monomeric material after folding was much higher for HS1S2I (~85%) than for HS1S2 (~30%). The K_d value of AMPA binding to folded HS1S2I was 9.9±1.9 nM. The IC_{50} values for glutamate and kainate were 760±76 and 11±2.2 μM, respectively.[17]

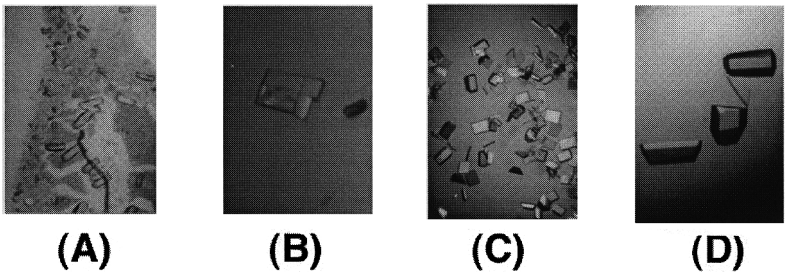

Figure 6. Comparison of crystals of S1S2 (A and B) and S1S2I (C and D). The crystals were grown in 4-μl hanging drops (see the Experimental). The reservoir solutions were (A) 10 mM glutamate, 0.1 M NaOAc, pH 6.0, 22.5% PEG 1K, 50 mM Li_2SO_4. (B) 10 mM kainate, 0.1 M NaOAc, pH 5.0, 21% PEG 3350, 200 mM $(NH_4)_2SO_4$. (C) 10 mM kainate, 50 mM potassium phosphate, pH 4.0, 12% PEG 8K; (D) 10 mM kainate, 50 mM potassium phosphate, pH 5.5, 13% PEG 8K.[17]

The stability of the shorter HS1S2I was significantly improved compared to the original HS1S2 construct. For example, in a limited trypsin digestion, the full-length HS1S2 was completely digested into fragments at a trypsin to protein ratio of 1:800. However, even at trypsin to protein ratio (weight:weight) of 1:200 no internal site in HS1S2I was cut. Equally significant differences in the sensitivity of HS1S2 and HS1S2I to chymotrypsin digestions were observed. In addition to the increase in protease resistance, HS1S2I was more thermally stable than HS1S2. For instance, HS1S2I retained 50% of its ^{3}H AMPA ligand binding activity after incubation at room temperature for two weeks. Under the same conditions, HS1S2 lost all measurable ligand binding activity. In terms of crystallization behavior, HS1S2I produced crystals with dimensions more than 0.2 mm that diffracted to 1.6 Å resolution using synchrotron radiation (Fig. 6). By contrast, the HS1S2 construct only gave micro crystals under optimized conditions.

Discussion

Most eukaryotic membrane proteins are difficult and expensive to over produce in multimilligram quantities. The iGluRs and their associated domains are no exception. Prior to our studies, facile and economical over production of the iGluR ligand binding core was not feasible.[15,23,24] For example, the initial efforts at over production of the ligand binding core of the GluR4 receptor yielded only ~0.1 mg of crude protein per liter of culture.[15] The strategy for over production of HS1S2 described here (Scheme 1) exploited the abundant expression of the GluR2 S1S2 protein in *E. coli* as inclusion bodies and the efficient in vitro folding of the partially purified, denatured protein.

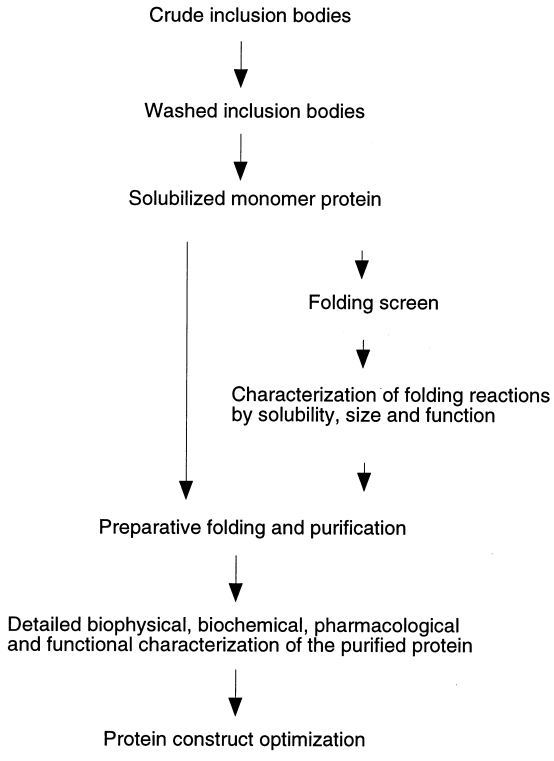

Scheme 1. The flow chart for the large scale production of GluR2-S1S2.

The major advantages of expression of a target protein as inclusion bodies in *E. coli* are as follows. (1) *E. coli* expression systems are relatively well understood, economical and allow for a rapid turn-around time. In addition, there are many choices of cloning and expression vectors and host cells.[25] (2) Proteins expressed as inclusion bodies are generally resistant to proteolytic degradation. (3) Isolation and partial purification of inclusion bodies are straightforward and easily scaled up, primarily because the protein of interest is typically the major component of the inclusion bodies. For example, expression of HS1S2 yielded 120~150 mg of inclusion bodies per liter of cell culture and the inclusion bodies were composed of ~80% HS1S2. Subsequent SEC purification of the inclusion body-derived material in Buffer A yielded about 100 mg of monomeric HS1S2.

The critical step of protein over production from inclusion body derived material is in vitro folding, a process which we refer to as preparative protein folding.[26,27] Although there have been many successful examples of preparative protein folding from inclusion bodies, the reported methods are often empirical and specific to individual proteins. There is no 'universal' condition for folding all proteins. The problem is that there are a number of factors that affect protein folding reactions and the impact of each factor on a different protein may vary. Examples of such factors are protein concentration, temperature, pH, ionic strength, polar additives, osmolytes, detergents, chaotropes, reducing or oxidizing agents, ligand, and the mode by which the denaturant concentration is reduced. In addition, proteinaceous chaperones may be employed to promote folding in vitro. Given so many factors, finding an effective condition for folding a particular protein may be difficult and time consuming. For instance, if 12 factors are considered and each factor has two levels, a total of 2^{12} or 4096 experiments would be required to evaluate all of the possible combinations.

In effort to over produce HS1S2, we have developed fractional factorial protein folding screens to answer the question of whether proteins derived from inclusion bodies can be folded into a biologically active conformation using a small number of experiments. As shown in the Experimental section, the initial folding screen included 12 factors, with each factor sampled at two levels. These parameters were then used in the design of a 16 experiment, resolution III fractional factorial folding screen; this first screen was subsequently improved to yield another, more generally useful screen.[28] On the basis of the initial screen, multiple conditions yielded folded HS1S2 protein. The modified folding screen has recently been shown to be useful for folding a kainate receptor S1S2 core, lysozyme, carbonic anhydrase and the extracellular domain of human fibroblast growth factor receptor (FGFR2).[28,29]

Inspection of the results from the folding screen indicates that the most important factors are temperature, pH and presence of arginine. Folding at low temperature and at high pH were clearly favored and inclusion of arginine at concentrations as high as 0.65 M also enhanced the folding process. In fact, quantitive analysis of the folding of related

S1S2 constructs have borne out this conclusion.[28] Low temperature is probably favorable because the protein is unstable at 20°C, high pH likely allows for facile rearrangement of disulfide bonds, and the inclusion of arginine helps minimize aggregation during folding.[26] Because the fractional factorial folding screen employed in this work only sampled a small portion of the possible folding conditions, as yet untested conditions present in the full factorial may prove superior. In principle, one can predict what conditions might prove most effective if one has determined the effects of each of the factors in the screen. At this juncture, we have optimized folding conditions not by predicting what additional conditions might be good, but rather by generating a new screen based on the 3 to 4 factors which have the greatest positive main effects, as determined from the initial screen.

Because the unfolded protein under native solution conditions tends to aggregate, analyzing protein solubility at the end of the folding reactions is a straightforward and easy way to quantify the folding process. Centrifugation or filtration of the folding reaction mixture removes the protein precipitate, thus enabling the analysis of the supernatant or filtrate by UV/Vis spectroscopy or SDS-PAGE. However, solubility under non-denaturing conditions is not a sufficient requirement for a correctly folded protein. For example, a misfolded protein can be soluble as a high aggregate at concentrations as high as 3 mg/ml.[30] A correctly folded protein should possess a well defined association state. To check the aggregation state, native PAGE[31] is particularly useful, especially because multiple samples can be analyzed in parallel. Analytical SEC is another straightforward approach to estimate the aggregation state and purity of the solubilized protein; in fact, SEC can be scaled up for preparative purification.[32] Dynamic light scattering is a third approach that has proven helpful for investigating the aggregation state of proteins and for estimating the degree of polydispersity.[33] Finally, analytical ultracentrifugation is the most reliable method to evaluate the size of proteins under non denaturing conditions but unfortunately it is also the most involved and requires sophisticated instruments.[34]

A functional assay is of great assistance in determining if a protein is correctly folded. For the HS1S2 construct, the functional assay included direct ^{3}H AMPA binding as well as competition for ^{3}H AMPA binding by glutamate and kainate. Not surprisingly, the folding conditions that gave the highest yield of monomer (2, 13 and 15) also had the highest ligand binding activity. Further investigation of the ligand binding activity of the folded HS1S2 showed that the folded material had a K_d value for AMPA binding and IC_{50} values for glutamate and kainate that were similar to the values obtained from a recombinant GluR2-S1S2 construct expressed in the *E. coli* periplasm[15] and from the intact receptor expressed in either insect cells[35] or human embryo kidney fibroblasts.[36] The differences in binding affinities of AMPA, glutamate and kainate between HS1S2 and HS1S2I may be related to the different protein conformational preference for various ligands and different conformational flexibility between the two protein constructs. The difference in the subdomain boundaries and the linker size between HS1S2 and HS1S2I may affect the free energy associated with protein conformational changes during ligand binding.[18,37]

Spectroscopic analysis often provides useful information about protein conformation and conformational changes. For example, the CD spectra of HS1S2 before and after folding were significantly different. The α-helix content estimated from the CD spectrum of the folded HS1S2 (35%) was indistinguishable from that shown in the crystal structure of GluR2-S1S2 (34.9%).[18] For fluorescence spectral analysis, addition of 1 mM glutamate or kainate to the HS1S2I solution resulted in a 1-nm red-shift of the emission λ_{max} and 4–14% emission intensity increases at 331 nm while the same concentration of alanine did not evoke such changes. Although these spectral changes are a consequence of local environmental changes of all tyrosine and tryptophan residues in the protein, a red-shift in the emission fluorescence spectrum is often related to differences in the solvent relaxation around the exited state dipole of tryptophan residues.[38] The differences in the fluorescence spectra of the apo and agonist-bound states may prove useful in subsequent studies of the relationships between ligand binding and conformational changes. For example, the protein confomational changes of the ligand binding dimain of GluR4 by ligand binding were monitored by changes in fluorescence emission intensity.[37] In the case of GluR4 ligand binding core, the protein flurescence emission intensity at 336 nm decreased upon ligand binding.[37] However, comparison between fluorescence changes of GluR2 and GluR4 ligand binding cores upon ligand binding may be complicated because of differences in the protein construct, buffer composition and the emission wavelength.

Limited proteolysis combined with subsequent MALDI-MS analysis is a useful approach to evaluate whether a protein is folded, to estimate the extent to which the population of protein molecules adopts a homogeneous conformation, and to provide information for new protein construct design.[39,40] Unfolded proteins or highly heterogeneous protein samples often result in either incomplete or random cleavage. In contrast, the limited digestion of folded and pure proteins typically results in the accumulation of proteolytic intermediates, which are the consequence of cleavages at termini and flexible loops. In the cases of either HS1S2 or HS1S2I, the His-tag was cleanly removed by limited thrombin or trypsin digestion, indicating that all of the protein molecules had uniformly accessible amino termini. The fact that the trypsinolysis fragments were stabilized by the presence of glutamate also supported the notion that the protein was properly folded.

For detailed biochemical, pharmaceutical and structural investigations, a stable protein construct is highly desirable. One approach to such constructs is to remove non-essential and flexible regions of the protein sequence. In optimizing the GluR2-S1S2 construct, we employed multiple sequence alignment and limited proteolysis results as guides to delete non-conserved and protease-accessible sequences. The optimized construct (HS1S2I) was more stable to thermal denaturation and proteolytic degradation and was more readily crystallized in comparison to the initial, longer construct.

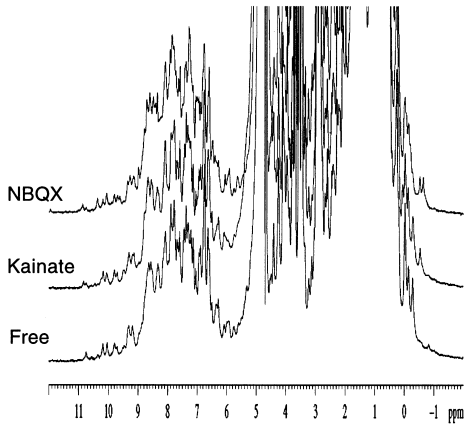

Figure 7. Comparison of the proton NMR spectra of GluR2-S1S2 in the free form and complexed to kainate and NBQX. The protein samples (0.5 mM) were prepared in a 50 mM phosphate buffer at pH 6.5. The spectra were collected on a Bruker DRX600 NMR spectrometer at 25°C.

The strategies for high level protein production described in this paper provided hundreds of milligrams of purified and active GluR2-S1S2 for detailed biochemical and crystallographic studies. Moreover, our methods for protein production can be applied to the preparation of material for NMR studies (Fig. 7) by taking advantage of the fact that *E. coli* can be grown in chemically defined media. The resulting ^{15}N- and ^{13}C-labeled proteins can then be used for detailed NMR investigations that range from studies of protein dynamics to drug discovery ventures.

Conclusion

Preparative folding from inclusion bodies provided an efficient way to produce large quantities of purified and active GluR2-S1S2. Discovery and improvement of the folding conditions were directed by a novel fractional factorial protein folding screen. The resulting folded GluR2-S1S2 constructs were then analyzed by biophysical, biochemical and functional approaches. By combining efficient expression and folding methods, biochemical and functional assays, and protein engineering approaches, we have developed useful methods to produce large quantities of active and stable GluR2-S1S2 for detailed structural, biochemical and functional studies.

Experimental

Plasmid construction

An expression vector, pETGQ, was constructed by modification of pET30b from Novagen (Madison, WI). Oligos were purchased from Operon (Almeda, CA). Restriction enzymes were from New England Biolabs (Beverly, MA). The sequences between Nde I and Nco I of pET30b were replaced by a sequence of 5′-TATGCACCATCATCATCATCATCATCACAGCAGCGGCCTGGTGCCGCGCGG-3′ and 5′-CATGGCGCTGCCGCGCGGCACCAGGCCGCTG-CTGTGATGATGATGATGATGATGGTGCA-3′ by cassette mutagenesis.[16] The Nco I and Xho I sites were used to clone the HS1S2 and HS1S2I genes. The HS1S2 gene was generated by PCRs using GluR2 cDNA (flop) as the template. PCRs were carried out on a GeneAmp PCR system 2400 (Perkin Elmer). Oligo #1 (5′-CCGCTCGAGTCATCAGTTGCTCAGACTGAGGGC-3′) and oligo #2 (5′-TTCTTCGGCATTGACCTCACCCT-CGGTCGACTCATAGGCTAAAGG-ATC-3′) were used as primers to produce the S1 gene fragment. Oligo #3 (5′-GAGGTCAATGCCGAAGAAGAGGGATTTGAGAG-GATGGTGTCTCCCATC-3′) and oligo #4 (5′-CCGCTCGAGTCATCAGTTGCTCAGACTGAGGGC-3′) were used to generate the S2 fragment. The HS1S2 gene was constructed by using the S1 and S2 fragments as templates and oligos #1 and #4 as primers. Cloning of the HS1S2 gene into pETGQ gave plasmid pHS1S2. The HS1S2I gene was constructed by deletion of the terminal sequences of S1 and S2 and modification of the linker region between S1 and S2 of pHS1S2. The deletion mutagenesis was performed by the following PCRs and subcloning steps. Primers PRMC1 (GAGTAGCCAGAGTCCGG) and PRMC2 (GCCCAAGCTTCTC-GAGTCAGCT-GCCG-CACTCTCCTTTG) were used to produce the C-terminal truncation of the S2 fragment, which was then cloned into the pHS1S2 plasmid using BamH I and Xho I sites to form pHS1S2C. Primers PRM1 (GGGCTACTGTG-TTGACTT) and PRMH2 (GTTACCATCAGTGCCTTTGGACTTCT-GAGGCTT) were used to generate deletions in the C-terminal sequences of S1 and the linker region. Primers PRMH3 (GGCACTGATGGTAACCCCATCGAAAGTGCTGA) and PRM4 (CTTCTGCGGTAGTCCTC) were used to produce deletion mutations in the linker region and the N-terminal sequences of S2. After gel purification, the above two PCR products were used as templates to generate a gene with deletions in the C-terminal sequences of S1, the linker region and the N-terminal sequences of S2. Subcloning of the truncated gene back to pHS1S2 using Pst I and Bgl II sites gave pHS1S2H. An additional subcloning step to replace the fragment between Bgl II and Xho I of pHS1S2H by the fragment between Bgl II and Xho I of pHS1S2C yielded the pHS1S2I plasmid.[17]

Protein expression and purification

A single colony of BL21(DE3) transformed with pHS1S2 or pHS1S2I was placed in 50 ml of LB medium supplemented with 30 μg/ml of kanamycin (LB_{kan}). The culture was shaken in a 37°C incubator overnight. The next day, one volume of the overnight culture was added to 100 volumes of fresh LB_{kan} and the resulting broth was incubated at 37°C for 3 h. Once the OD_{600} reached 0.6, IPTG was added to 1 mM and the culture was shaken for an additional 2 h. The cells were then collected by centrifugation. The cells from one liter of culture were resuspended in 9 ml of Buffer C (50 mM Tris-HCl, 1 mM EDTA, 100 mM NaCl, pH 8.0, 1 mM PMSF, 0.5 mg/ml lysozyme, 1.2 mg/ml deoxycholate, 0.1 mg/ml of DNase I). The cell suspension was passed through a French Press two times and the cell lysate was centrifuged at 25000×g for 30 min. The pellet was resuspended in 20 ml of Buffer D (50 mM Tris-HCl, 10 mM EDTA, 100 mM NaCl, 0.5% Triton X-100, 1 mM PMSF) at 4°C for 2 h and then centrifuged again to pellet the inclusion body materials. The pellet was next washed with 20 ml of Buffer B supplemented with 1 mM PMSF. The washed inclusion bodies were solubilized in 9 ml of Buffer

E (50 mM Tris-HCl, pH 7.4, 5 mM EDTA, 8 M GuHCl, 50 mM DTT) at rt (~4 h). The residual insoluble materials were removed by centrifugation at 125000×g (20°C, 1 h). The supernatant was then dialyzed against 10 volumes of Buffer A at 4°C for 2 h, and the dialyzed material was clarified by centrifugation at 125000×g (4°C, 1 h). For SEC purification, a XK 26/70 Superose 12 column was equilibrated with Buffer A, the solubilized HS1S2 was concentrated to about 40 mg/ml and 2 ml of the concentrated material was loaded onto the SEC column. The major protein peak fractions were pooled for folding reactions. In larger scale preparations, the SEC purification step was omitted.

Design of protein fractional factorial folding screen

A resolution III folding screen composed of the 12 factors, each sampled at 2 levels, was designed using JMP software. The factors and the '+' and '−' levels were: (1) protein concentration: 1.0, 0.1 mg/ml; (2) pH: 8.5, 6.0; (3) T: 20, 4°C; (4) divalents: 2 mM $CaCl_2$ plus 2 mM $MgCl_2$, 1 mM EDTA; (5) arginine: 0.0, 0.5 M; (6) osmolytes: 0.0, 20% glycerol plus 1% sucrose; (7) GuHCl: 0.0, 0.75 M; (8) redox conditions: 1 mM GSH plus 0.1 mM GSSG, 1 mM DTT; (9) detergent: 0.0 mM, 5 mM DiC_7PC; (10) ligand: 0.0, 10 mM glutamate; (11) PEG 3350: 0.0%, 0.05%; (12) ionic strength: 10 mM NaCl plus 0.2 mM KCl, 250 mM NaCl plus 5 mM KCl. The fractional factorial folding screen was composed of 16 conditions (Table 1). For HS1S2I folding reactions, a new folding screen (Table 2) using a narrower pH range (pH 7 and 8.5) and variations in arginine, GuHCl, NaCl and KCl concentrations was designed based on the folding results of HS1S2.

The folding screen reactions were carried out by dialyzing 0.2 ml of the purified monomeric HS1S2 in buffer A against 20 ml of each of the 16 folding buffers (Table 1). The next day, the folding reaction mixtures were dialyzed against 25 volumes of Buffer B. The dialysis buffer was changed 4 times. The folding reaction mixtures were then centrifuged at 128000×g at 4°C for 30 min. The supernatant was saved for SDS-PAGE, SEC and ligand binding analysis.

Size exclusion chromatography

For HPLC size exclusion chromatography (SEC), a TSK-GEL G3000SW column (TosoHaas, Montgomeryville, PA) was equilibrated in buffer F (0.1 M sodium phosphate, pH 6.8, 200 mM Na_2SO_4, 1 mM DTT, 10 mM glutamate, 2 mM EDTA). The column was calibrated with apoferritin (443 kDa), β-amylase (200 kDa), alcohol dehydrogenase (150 kDa), bovine serum albumin (66 kDa) and carbonic anhydrase (29 kDa). The flow rate was 0.75 ml/min. The loading volume was 50 μl. For FPLC SEC purification, a XK 26/100 Superose 12 column was equilibrated with Buffer B. The column was run at a flow rate of 2 ml/min at 4°C.

Spectroscopic measurements

Fluorescence spectra were measured on an AB2 fluorescence spectrophotometer at room temperature. The excitation wavelength was 280 nm. The HS1S2I concentration was 1.2 μM in Buffer B. The ligand concentrations were 1 mM. Circular dichroism (CD) spectra were measured on a JASCO J-600 spectropolarimeter. The HS1S2 concentration was 1.0 mg/ml. The buffer for native conditions was Buffer B with 1 mM DTT and 10 mM glutamate. The denaturing buffer was Buffer A.

Ligand binding measurements

Ligand binding reactions were carried out in Buffer G (30 mM Tris–HCl, 100 mM KSCN, 2.5 $CaCl_2$, 10% glycerol, pH 7.2) in a total volume of 500 μl on ice for 1 h.[14,16] For K_d measurements, the protein concentration was 0.8 μg/ml. The commercial ^3H AMPA was diluted with cold AMPA to make a 1 μM solution with specific activity of 10.6 Ci/mmole. The final AMPA concentrations were 1, 3, 10, 50, 100 and 200 nM. For IC_{50} measurements, the reaction mixtures were made up of 0.2 μg/ml protein, 10 nM ^3H AMPA (53 Ci/mmole) and different concentrations of cold ligand (10^{-4}–10^{-9} M for glutamate, 10^{-3}–10^{-8} M for kainate). GSWP 02500 membranes were used for the ligand binding measurements. The membranes were wetted with Buffer G and loaded onto a filter manifold connected to a vacuum line. After the reaction mixtures were loaded and sucked through the membranes, the membranes were washed with 2 ml of ice cold Buffer G (3 times). The washed membranes were transferred into a 7-ml scintillation vials and 6 ml of scintillation liquid was added. After incubation at rt for at least 2 h to solubilize the bound ^3H AMPA, the radioactivity was measured on a Beckman liquid scintillation counter. The K_d and IC_{50} measurements were carried out in triplicate and duplicate, respectively. The data was analyzed using a PRISM nonlinear curve fitting program.

Proteolysis, N-terminal sequence and Maldi-MS analysis

Trypsin and chymotrypsin digestion reactions were carried out in Buffer H (20 mM Tris-HCl, 10 mM $CaCl_2$, 100 mM NaCl, pH 8) at room temperature for 40 min. The protein concentration was 1.5 mg/ml. The trypsin concentrations ranged from 0.5 to 15 μg/ml. The chymotrypsin concentrations ranged 0.02 to 0.3 U/ml. The reactions were stopped by 1 mM PMSF. The digestion products were analyzed by SDS-PAGE. Maldi-MS and N-terminal sequence analyses were performed by the Protein Core Facility at Columbia University. For N-terminal sequence analysis of the proteolysis products, the protein bands on the SDS-PAGE gel were transferred onto an Immobin-pSQ membrane in Buffer I (10 mM 3-[cyclohexylamino]-1-propane sulfonic acid, 10% methanol, pH 11). The transfer was carried out at 12 V at rt for 2 h using a protein transfer device (IDEA Scientific Company). The transferred membrane was washed with Milli-Q water for 5 min, stained with 0.25% Coomassie Blue R-250 in 40% methanol for 15 min, and destained in 50% methanol. The protein bands containing 1–10 μg of proteins were cut out from the membrane and sent for N-terminal sequence analysis.

Protein crystallization

The Hampton Crystal Screen Kits were employed to search for initial crystallization conditions. The initial

PEG crystallization conditions were optimized by varying PEG molecular weight, PEG concentrations, pH values and salt concentrations. In the crystallization screen experiments, the hanging drops were composed of 1 μl of the protein solution and 1 μl of the reservoir solution. The reservoir solution volume was 500 μl. Two protein concentrations (7.5 and 15 mg/ml, before mixing) were used under each reservoir solution condition. The crystallization trays were incubated in a 4°C incubator. For preparative crystallization, the hanging drops were composed of 2 μl of the protein solution and 2 μl of reservoir solution. The X-ray diffraction data were collected at Columbia University, CHESS, the National Synchrotron Light Source and the Advanced Photon Source.

Acknowledgements

Drs Hartley and Heinemann are acknowledged for providing the rat GluR2 clone. We would like to thank Mr Sun and Mr Jin for cloning and ligand binding experiments of the HS1S2I construct, Ms Gawinowicz for N-terminal sequence and MALDI-MS analyses and Dr Ming-Ming Zhou for the NMR spectra. We are also grateful to Drs Karlin, Javitch, Hendrickson, Hirsh, Palmer, Pyle, and Thanos for their helpful assistance and for equipment use. Support for this research was provided by a NSF Young Investigator Award, an Alfred P. Sloan Research Fellowship, the Klingenstein Foundation and the National Alliance for Research on Schizophrenia and Depression.

References

1. Dingledine, R.; Borges, K.; Bowie, D.; Traynelis, S. F. *Pharmacol. Rev.* **1999**, *51*, 7–61.
2. Dingledine, R.; McBain, C. J.; McNamara, J. O. *Trends Pharmacol. Sci.* **1990**, *11*, 334–338.
3. Beal, M. F. *FASEB J.* **1992**, *6*, 3338–3344.
4. Watkins, J. C.; Krogsgaard-Larsen, P.; Honoré, T. *Trends Pharmacol. Sci.* **1990**, *11*, 25–33.
5. Donevan, S. D.; Rogawski, M. A. *Neuron* **1993**, *10*, 51–59.
6. Zorumski, C. F.; Yamada, K. A.; Price, M. T.; Olney, J. W. *Neuron* **1993**, *10*, 61–67.
7. Hollmann, M.; Heinemann, S. *Annu. Rev. Neurosci.* **1994**, *17*, 31–108.
8. Stern-Bach, Y.; Bettler, B.; Hartley, M.; Sheppard, P. O.; O'Hara, P. J.; Heinemann, S. F. *Neuron* **1994**, *13*, 1345–1357.
9. Wo, Z. G.; Oswald, R. E. *Proc. Natl. Acad. Sci. USA* **1994**, *91*, 7154–7158.
10. Hollmann, M.; Maron, C.; Heinemann, S. *Neuron* **1994**, *13*, 1331–1343.
11. Bennett, J. A.; Dingledine, R. *Neuron* **1995**, *14*, 373–384.
12. Kuusinen, A.; Abele, R.; Madden, D. R.; Keinänen, K. *J. Biol. Chem.* **1999**, *274*, 28937–28943.
13. Leuschner, W. D.; Hoch, W. *J. Biol. Chem.* **1999**, *274*, 16907–16916.
14. Kuusinen, A.; Arvola, M.; Keinänen, K. *EMBO J.* **1995**, *14*, 6327–6332.
15. Arvola, M.; Keinänen, K. *J. Biol. Chem.* **1996**, *271*, 15527–15532.
16. Chen, G. Q.; Gouaux, E. *Proc. Natl. Acad. Sci. USA* **1997**, *94*, 13431–13436.
17. Chen, G. Q.; Sun, Y.; Jin, R.; Gouaux, E. *Protein Sci.* **1998**, *7*, 2623–2630.
18. Armstrong, N.; Sun, Y.; Chen, G. Q.; Gouaux, E. *Nature* **1998**, *395*, 913–917.
19. Andrade, M. A.; Chacón, P.; Merelo, J. J.; Morán, F. *Protein Eng.* **1993**, *6*, 383–390.
20. Merelo, J. J.; Andrade, M. A.; Prieto, A.; Morán, F. *Neurocomputing* **1994**, *6*, 443–454.
21. Sutcliffe, M. J.; Wo, Z. G.; Oswald, R. E. *Biophys. J.* **1996**, *70*, 1575–1589.
22. Reeke, G. N. J.; Becker, J. W.; Edelman, G. M. *J. Biol. Chem.* **1975**, *250*, 1525–1547.
23. Bettler, B.; Boulter, J.; Hermans-Borgmeyer, I.; O'Shea-Greenfield, A.; Deneris, E. S.; Moll, C.; Borgmeyer, U.; Hollmann, M.; Heinemann, S. *Neuron* **1990**, *5*, 583–595.
24. Kuusinen, A.; Arvola, M.; Oker-Blom, C.; Keinänen, K. *Eur. J. Biochem.* **1995**, *233*, 720–726.
25. Goeddel, D. V. Gene Expression Technology; In *Methods in Enzymology*; Abelson, J. N., Simon, M. I., Eds.; Academic: Pasadena, CA, 1990; Vol. 185, pp 11–195.
26. Rudolph, R.; Lilie, H. *FASEB J.* **1996**, *10*, 49–56.
27. Guise, A. D.; West, S. M.; Chaudhuri, J. B. *Mol. Biotechnol.* **1996**, *6*, 53–64.
28. Armstrong, N.; Lencastre, A. D.; Gouaux, E. *Protein Sci.* **1999**, *8*, 1475–1483.
29. Stauber, D. J.; DiGabriele, A. D.; Hendrickson, W. A. *Proc. Natl. Acad. Sci. USA* **2000**, *97*, 49–54.
30. Chen, G. Q.; Gouaux, J. E. *Protein Sci.* **1996**, *5*, 456–467.
31. Coligan, J. E.; Dunn, B. M.; Ploegh, H. L.; Speicher, D. W.; Wingfield, P. T. In *One-dimensional electrophoresis using non-denaturing conditions*. *Current Protocols in Protein Science*; Chanda, V. B. Ed.; Wiley: USA, 1995; pp 10.3.1–10.3.11.
32. Coligan, J. E.; Dunn, B. M.; Ploegh, H. L.; Speicher, D. W.; Wingfield, P. T. Gel-filtration chromatography. In *Current Protocols in Protein Science*; Chanda, V. B., Ed.; Wiley: USA, 1995; pp 8.3.1–8.3.30.
33. Ferré-D'Amaré, A. R.; Burley, S. K. Dynamic light scattering in evaluating crystallizability of macromolecules; In *Methods in Enzymology*, Carter, J. C. W., Sweet, R. M., Eds.; Academic: New York, 1997; Vol. 276, pp 157–166.
34. Laue, T. M.; Stafford, W. F. *3rd Annu. Rev. Biophys. Biomol. Struct.* **1999**, *28*, 75–100.
35. Keinänen, K.; Köhr, G.; Seeburg, P. H.; Laukkanen, M.-L.; Oker-Blom, C. *Bio/Technology* **1994**, *12*, 802–806.
36. Keinänen, K.; Wisden, W.; Sommer, B.; Werner, P.; Herb, A.; Verdoorn, T. A.; Sakmann, B.; Seeburg, P. H. *Science* **1990**, *249*, 556–560.
37. Abele, R.; Keinänen, K.; Madden, D. R. *J. Biol. Chem.* **2000**, *275*, 21355–21363.
38. Royer, C. A. Fluorescence Spectroscopy; In *Protein Stability and Folding: Theory and Practice*, Shirley, B. A., Ed.; Humana: Totwa, NJ, 1995; Vol. 40, pp 65–89.
39. Cohen, S. L.; Ferré-D'Amaré, A. R.; Burley, S. K.; Chait, B. T. *Protein Sci.* **1995**, *4*, 1088–1099.
40. Cohen, S. L. *Structure* **1996**, *4*, 1013–1016.